Wave function for spontaneous parametric down-conversion with orbital angular momentum

Geraldo A. Barbosa*
Department of Electrical Engineering and Computer Science, Northwestern University, 2145 N. Sheridan Road, Evanston, Illinois 60208-3118, USA
(Received 16 July 2009; published 14 December 2009)

Several wave-function approximations describing spontaneous parametric down-conversion can be found in the literature. Basically all cases are derived from the standard Hamiltonian for parametric down-conversion. Most frequently, particular cases describing collinear or paraxial approximations are described. This work presents a wave function in compact form, valid for all cases of single photon-pair conversion (Type I or Type II), for all angles allowed by the phase-matching conditions and for all orbital angular momentum values l. Examples are given of coincidence structures to be expected for signal and idler photons. Partial transfer of orbital angular momentum from the pump laser to the photon pair is discussed. Some hypothesis for the decay channels of the nontransferred part of the orbital angular momentum is made.

DOI: 10.1103/PhysRevA.80.063833 PACS number(s): 42.65.Lm, 42.50.Dv, 42.50.Tx

I. INTRODUCTION

What is the wave function describing entangled photons from the spontaneous parametric down-conversion (SPDC) carrying orbital angular momentum (OAM)? The literature presents some answers to this question (e.g., [1–3]) and even include some controversies (e.g., [4]) that stress the fact that the current understanding of the phenomenon is still incomplete. In view of the nonuniformity on the current understanding, this work emphasizes some advantages and generality of a particular wave-function appropriate for SPDC with OAM. This derivation starts from a standard linear Hamiltonian and adds a small nonlinear contribution as a perturbation. Starting from fundamental principles may turn out to be necessary to achieve a full understanding of OAM's partial or nontransfer cases due to the light-matter interaction lacking azimuthal asymmetry. All steps in the derivation of the wave function were detailed and an analytical improvement over the wave function in [1] was achieved. Instead of a Laguerre polynomial that connects transversal properties of the entangled photons, a different polynomial was found, with the same order as the Laguerre one and overall factors but with different coefficients. A more reliable wave state was then obtained. With the single assumption of the crystal thickness smaller than the pump laser Rayleigh range, the obtained wave function is reduced to a very simple form. The path is then open for further advances as pointed along the paper.

An effort to improve the SPDC's wave function is worthwhile due to the importance of entanglement both for fundamental enquiries as well as for the broad applicability of these states to quantum information. In particular, customized states can be engineered with a better knowledge of the SPDC wave functions: e.g., refined interferences from distinct sources can be constructed or detection systems could be tailored to best use the available signals. Even analysis of photon-pair correlations at the source itself (see a first example in [5]) could profit from the knowledge of a general wave function describing SPDC. Whenever charge-coupled device arrays with true single-photon sensitivities *and* low noise appear in the market, instead of the current use of two directions to detect the entangled photon-pair, the whole SPDC emission ring(s) could be explored resulting in systems with shorter collection times. The entanglement of microscopic mechanical bodies through light-matter interaction using entangled OAM entangled signal and idler photons from SPDC could provide new possibilities in the field. General treatments for these problems are important as well as a general wave function for SPDC, that could cover almost all cases treated so far.

This paper briefly reviews the standard Hamiltonian describing SPDC, improves the wave function described in [1] and adds arguments pointing cases where partial transfer of OAM between pump photons and down-converted photons is to be expected. Phase match conditions are sketched, with references to [3]. The discussion on OAM losses to the medium is advanced. Suggestions are then made about improving the current understanding of these losses either by a macroscopic approach or by modifications of the standard Hamiltonian to include the microscopic OAM decay channels. Both theoretical and experimental works are still needed to achieve a full understanding of OAM transfer in SPDC.

II. HAMILTONIAN

SPDC is a nonlinear process, where single photons from a pump laser at frequency ω_p—usually at ultraviolet frequencies—may excite a nonlinear crystal, or an amorphous medium, nonresonantly, in a virtual process. After each successful single-photon excitation, the medium decays within a very short time ($\Delta t \to 0$), due to this virtual character. The excited medium's energy usually decays either into the energies of two simultaneous photons, arbitrarily called signal or idler or into a pump beam photon. It has usually been assumed that no energy, momentum, or orbital angular momentum is taken by the medium in the down-conversion process. By itself, the Hermitian nature of the accepted Hamiltonian implies a lossless process. This understanding contributed for the current modeling of the SPDC processes where the pump intensity is *low* and at each excitation of the

*g-barbosa@northwestern.edu

crystal by a pump photon, no signal or idler photon is present. The decaying processes are then considered to be produced by random vacuum field fluctuations or, using an old jargon, produce "amplification of vacuum quantum noise." Any photon-pair created is described by an *entangled* state. This entanglement includes properties such as energy, linear momentum, orbital angular momentum, polarization, and so on. Each single *pair* emission occurs in a random time and, in the general case, along two conjugated directions that cannot be *a priori* predicted. This implies that the light state of the process is a coherent superposition of all possible photon-pair emissions, expressed as a *sum* over all possible decays. The succession of decays produces a spectacular rainbow of colors, due to the possibility of a continuum for the signal and idler energies, only constrained by their sum being equal to the energy of the pump photon and satisfying the hypothesis of a nonabsorptive medium.

The timed detection of photon pairs in SPDC has to be explained by multimode theories, due to the necessity of constructing localized wave packets. Frequently used single mode theories, associated with infinite size wave packets, predict a uniform time detection probability to find photons in the field—not the localized conjugated photons detected in coincidence measurements. Since seminal works developed in the 1960s [6], multimode theories, e.g., [7], have been established and account for most of the basic features seen in SPDC.

Some questions will be raised ahead indicating that SPDC with OAM bring new elements to this scenery and may need the inclusion of new aspects to provide a complete description of the phenomenon.

A. Weak nonlinear interaction

Electric fields in the neighborhood of molecules or atoms can be quite intense, of order of a few volts per Å, or $E \sim 10^8$ V/m. A pulsed laser may produce intense fields (a light power of 1 MW/mm^2 gives $E \sim 3 \times 10^7$ V/m) inducing appreciable nonlinear effects. In this regime, molecules are deformed either in a reversible or irreversible ways [8], beyond Hooke's limit, or linear limit. CW lasers, of lower power ($P=100$ mW in 1 mm^2 would give $E \sim 10^0$ V/m), lead to weak nonlinear effects and, consequently, first-order terms in a perturbation theory will suffice to take care of the induced polarizability. In the range of weak fields the medium polarization can be written [9]

$$P_i = \int_0^\infty \chi_{ij}^{(1)}(t') E_j(\mathbf{r}, t-t')dt' + \int_0^\infty \int_0^\infty \chi_{ijk}^{(2)}(t',t'') E_j(\mathbf{r}, t-t') \times E_k(\mathbf{r}, t-t'')dt'dt'', \quad (1)$$

where $\chi^{(1)}$ and $\chi^{(2)}$ are the first- and second-order electrical susceptibilities. For crystals *without* inversion symmetry centers [10], $\chi^{(2)} \neq 0$. The time dependence in the integrals show that retarded effects could contribute to the polarization and a simple dependence on the position was written implying local responses—a simplification. Other usual simplifications are low absorption and low dispersion at the involved wavelengths.

Classically, the linear part of electromagnetic energy density in matter is [9]

$$u = \frac{1}{2}(\mathbf{D}\cdot\mathbf{E} + \mathbf{B}\cdot\mathbf{H}), \quad (2)$$

where $\mathbf{D}$ is the electric displacement vector and $\mathbf{B}$ is the magnetic field. One may rewrite the *linear* term of the electromagnetic energy in a Hamiltonian form,

$$\hat{\mathcal{H}}_0 = \frac{1}{2}\int_{V_I} (\hat{\mathbf{D}}\cdot\hat{\mathbf{E}} + \hat{\mathbf{B}}\cdot\hat{\mathbf{H}})d\mathbf{r}, \quad (3)$$

where V_I is the interaction volume. The small nonlinear term is added as a perturbation $\hat{\mathcal{V}}$ to $\hat{\mathcal{H}}_0$,

$$\hat{\mathcal{V}} = \frac{1}{2}\int_{V_I} \hat{\mathbf{E}}\cdot\hat{\mathbf{P}}^{NL}d\mathbf{r} = \frac{1}{2}\int_{V_I} \hat{E}_i(\mathbf{r},t)\int_0^\infty\int_0^\infty \chi_{ijk}^{(2)}(t',t'') \times \hat{E}_j(\mathbf{r},t-t')\hat{E}_k(\mathbf{r},t-t'')dt'dt''d\mathbf{r}. \quad (4)$$

The electric field operator in the medium can be written

$$\hat{\mathbf{E}}(\mathbf{r},t) = \hat{\mathbf{E}}^-(\mathbf{r},t) + \hat{\mathbf{E}}^+(\mathbf{r},t), \quad (5)$$

where

$$\hat{\mathbf{E}}^+(\mathbf{r},t) = [\hat{\mathbf{E}}^-(\mathbf{r},t)]^\dagger = \frac{1}{\sqrt{V}}\sum_{\mathbf{k},s} \mathbf{e}_{\mathbf{k},s} l(\omega)\hat{a}_{\mathbf{k},s}e^{i(\mathbf{k}\cdot\mathbf{r}-\omega t)}, \quad (6)$$

and $\mathbf{e}_{\mathbf{k},s}$ indicates mode polarization, V is the quantization volume, $\hat{a}_{\mathbf{k},s}$ is the annihilation operator and

$$l_\omega = i\left[\frac{\hbar\omega(\mathbf{k},s)}{2\varepsilon_0 n^2(\mathbf{k},s)}\right]^{1/2}. \quad (7)$$

Substituting the electric field, Eq. (6), in $\hat{\mathcal{H}}_0$ and in the nonlinear part of the energy, written as $\hat{\mathcal{V}}$, it follows

$$\hat{\mathcal{H}} = \hat{\mathcal{H}}_0 + \hat{\mathcal{V}}, \quad (8)$$

where

$$\hat{\mathcal{H}}_0 = \sum_{\mathbf{k}_j,s_j} \hbar\omega_j \hat{a}^\dagger_{\mathbf{k}_j,s_j}\hat{a}_{\mathbf{k}_j,s_j} (j=1,2,3) \quad (9)$$

$$\hat{\mathcal{V}} = \frac{1}{V^{3/2}}\sum_{\mathbf{k}_1,s_1}\sum_{\mathbf{k}_2,s_2}\sum_{\mathbf{k}_3,s_3} l^*_{\omega_1} l^*_{\omega_2} l_{\omega_3}\hat{a}^\dagger_{\mathbf{k}_1,s1}\hat{a}^\dagger_{\mathbf{k}_2,s2}\hat{a}_{\mathbf{k}_3,s_3} \times e^{i(\omega_1+\omega_2-\omega_3)t}[\tilde{\chi}^{(2)}_{ijk}(\mathbf{e}_{\mathbf{k}_3,s_3})_i(\mathbf{e}_{\mathbf{k}_1,s_1})^*_j(\mathbf{e}_{\mathbf{k}_2,s_2})^*_k] \times \int_{V_I} e^{-i(\mathbf{k}_1+\mathbf{k}_2-\mathbf{k}_3)\cdot\mathbf{r}}d\mathbf{r} + \text{H.c.}, \quad (10)$$

and H.c. indicates the Hermitian conjugated of the first term and

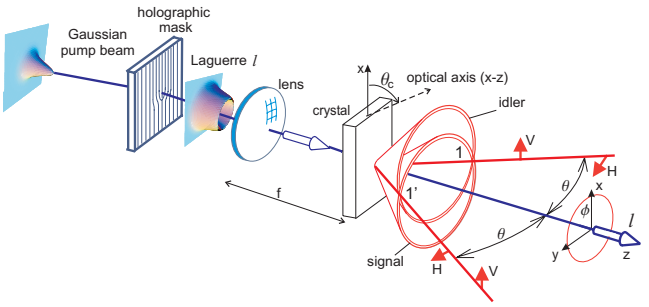

FIG. 1. (Color online) A nonlinear crystal is pumped by a laser beam carrying OAM. A signal and idler photon pair is created in a Type-II geometry. The pair can appear at any phase-matching region depicted as two cones. Pair of photons from positions 1 and 1′ are entangled in energy, momentum, and polarization. z is the quantization axis.

$$\tilde{\chi}^{(2)}_{ijk} \equiv \int_0^\infty \int_0^\infty \chi^{(2)}_{ijk}(t',t'')e^{i(\omega' t' + \omega'' t'')}dt'\,dt''. \tag{11}$$

V_I is the nonlinear interaction volume. Note that the indices 1, 2, and 3 are denoting signal, idler, and pump laser, respectively; other indices will be used along the paper, substituting 1, 2, and 3.

B. Hamiltonian

The interaction Hamiltonian (12), obtained from the above equations, has been accepted as a starting point to obtain the wave function.

$$\begin{aligned}\hat{H}_I = &\sum_{\sigma,\sigma'} \int d^3k d^3k' l^{(*)}_{\omega_{\mathbf{k}}} l^{(*)}_{\omega'_{\mathbf{k}}} \hat{a}^\dagger(\mathbf{k},\sigma)\hat{a}^\dagger(\mathbf{k}',\sigma') \\ &\times e^{i(\omega_{\mathbf{k}}+\omega_{\mathbf{k}'})t}\chi_{qjk}(\mathbf{e}_{\mathbf{k},\sigma})^*_j(\mathbf{e}_{\mathbf{k}',\sigma'})^*_k \\ &\times \int_{V_I} d^3r[\mathbf{E}_P(\mathbf{r},t)]_q e^{-i(\mathbf{k}+\mathbf{k}')\cdot\mathbf{r}} + \text{H.c.}\end{aligned} \tag{12}$$

$\mathbf{E}_P(\mathbf{r},t)$ is the electrical field associated with the pump beam, $\mathbf{k}$ and $\mathbf{k}'$ indicate signal and idler wave vectors and indices (σ,σ') represent possible polarization states. Repeated indices q, j, and k imply summations.

The lack of high efficiency media has been restricted most of the wave vector derivations to their first-order expansion through the evolution operator. In the wave vector description, this first-order expansion gives [11]

$$\begin{aligned}|\psi(t)\rangle = |0\rangle + \sum_{\sigma,\sigma'} \int d^3k' \int d^3k A_{\mathbf{k},\sigma;\mathbf{k}',\sigma'} l^{(*)}_{\omega_{\mathbf{k}},E} l'^{(*)}_{\omega_{\mathbf{k}'},E} \\ \times T(\Delta\omega)\tilde{\psi}_{lp}(\Delta\mathbf{k})\hat{a}^\dagger(\mathbf{k},\sigma)\hat{a}^\dagger(\mathbf{k}',\sigma')|0\rangle.\end{aligned} \tag{13}$$

$A_{\mathbf{k},\sigma;\mathbf{k}',\sigma'} = \chi^{(2)}_{1jk}[(\mathbf{e}_{\mathbf{k},\sigma})^*_j(\mathbf{e}_{\mathbf{k}',\sigma'})^*_k + (\mathbf{e}_{\mathbf{k}',\sigma'})^*_j(\mathbf{e}_{\mathbf{k},\sigma})^*_k]$ is the amplitude of the nonlinear polarizability, that depends on the unitary polarization vectors (σ polarized) as well as on the nonlinear susceptibility (see Ref. [3] for a detailed calculation). $T(\Delta\omega) = \exp[i\Delta\omega(t - t_{int}/2)]\sin(\Delta\omega t_{int}/2)/(\Delta\omega/2)$ is the time window function defining the $\Delta\omega$ range given the interaction time t_{int}, $\Delta\omega = \omega_{\mathbf{k}} + \omega'_{\mathbf{k}} - \omega_P$, $\Delta\mathbf{k} = \mathbf{k} + \mathbf{k}' - \mathbf{k}_P$. For $t_{int} \to \infty$, $T(\Delta\omega) \to \pi\delta(\Delta\omega)$. $\tilde{\psi}_{lp}(\Delta\mathbf{k}) = \int_{V_I} d^3r \psi_{lp}(\mathbf{r})\exp(-i\Delta\mathbf{k}\cdot\mathbf{r})$ and ψ_{lp} is the field amplitude in $\mathbf{E}(\rho,\phi,z;t) = \psi_{lp}(\mathbf{r})e^{i(k_P z - \omega_P t)}\hat{\mathbf{e}}$.

$\tilde{\psi}_{lp}(\Delta\mathbf{k})$ is an effective Fourier transform of the pump field, over the illuminated (x,y,z) volume, written in the reciprocal space variables $\mathbf{k}$, $\mathbf{k}'$ and with a phase modulation in $\mathbf{k}_P$. It may be seen as a core part of the wave function. For a pump beam with orbital angular momentum l one has [12]

$$\begin{aligned}\psi_{lp}(\rho,\phi,z) = &\frac{A_{lp}}{\sqrt{1+(z/z_R)^2}}\left[\frac{\rho\sqrt{2}}{w(z)}\right]^l L^p_l\left(\frac{2\rho^2}{w(z)^2}\right) \\ &\times \exp\left[-\frac{\rho^2}{w(z)^2}\right] \\ &\times \exp\left[-i\left(\frac{k\rho^2 z}{2(z^2+z_R^2)} + l\arctan(y/x)\right)\right] \\ &\times \exp[i(2p+l+1)\arctan(z/z_R)].\end{aligned} \tag{14}$$

L^p_l is the associated Laguerre polynomial and $\rho^2 = x^2 + y^2$. $w(z)$ is the beam waist in a generic position z; z_R is the Rayleigh range. $\tilde{\psi}_{lp}(\Delta\mathbf{k})$ has been frequently calculated under drastic simplifications and, therefore, with a limited range of validity. Many toy models have been used to capture certain features of interest for a given argument or application but a complete solution has not yet been obtained. However, the task does not seems unsurmountable. This work is one more step in this direction.

Besides the need of a general solution, to achieve results broadly valid, one has to insert parallel information such as first and higher order dielectric susceptibilities for the medium in question. The difficulties to derive susceptibilities from first principles led to the adoption of parametric descriptions obtained from experiments (e.g., Sellmeier indices). This interconnection of basic principles and parametric information from condensed matter is always present in the phase-matching conditions.

Figure 1 depicts a Type-II SPDC process where a nonlinear crystal is pumped by a laser mode carrying OAM. An initial Gaussian mode laser beam passes through a holographic mask creating the OAM beam. Just the degenerate signal and idler directions $(1,1')$ are shown. The full spectrum of SPDC is given by the superposition of OAM states shown in Eq. (13).

As discussed in the literature [1], there are conditions under which OAM from the pump beam is transferred to the SPDC photons. There are also cases where this transfer seems incomplete or frustrated. One may wonder if the Hamiltonian itself should be modified to lead to a complete explanation of the OAM transfer channels within the condensed matter. SPDC happens through a virtual interaction with electrons in condensed matter, with light propagating within the transparent band gap of the material. As causality

imposes a fast absorption or re-emission by the medium, perhaps these virtual electrons could play an intermediation role and involve phonons or rotorlike excitations to exchange OAM in the frustrated light-to-light process. In this case, in principle, it would be possible to detect OAM-excited states in the medium caused by the electrons unable to be de-excited onto photon pairs. These OAM-excitation states may be more easily seen at low temperatures where thermally excited phonon states are practically nonexistent. Anyway, the understanding of OAM transfer from pump photons to entangled photon states is still incomplete and the understanding of the underlying microscopic physics may be necessary to fully explain the phenomenon.

III. WAVE FUNCTION IN k SPACE

Calculation of $\tilde{\psi}_{lp}(\Delta\mathbf{k})$ in Eq. (13) is the first step to obtain a general wave function from the Hamiltonian (12). Appendix details the calculation and uses a single simplification expressed by $z/z_R \ll 1$. This is equivalent to $l_c/z_R \ll 1$ (l_c is the crystal thickness along the pump laser z propagation), because the variable z spans the illuminated crystal volume. This condition is almost standard in the experiments reported so far. The obtained solution is then quite general. The case $l_c/z_R \ll 1$ gives (Appendix)

$$\tilde{\psi}_{lp}(\Delta\mathbf{k}) = A_{lp}\pi l_c(-1)^l\left[\frac{k_P}{2z_R}\right]^{(l/2)-1}\frac{(l+p)!}{l!\,p!} \times \frac{\sin[l_c(\Delta k_z/2)]}{[l_c(\Delta k_z/2)]}\xi^{l/2}\mathcal{G}_l^p(\xi) \times e^{i(l\pi/2+l_c\Delta k_z/2-l\ \arctan(\Delta k_y/\Delta k_x)-(l_c+2z_0)\Delta k_z/2)}, \tag{15}$$

where ξ is the two-point transverse coordinate

$$\xi = \frac{z_R}{k_P}(\Delta k_x^2+\Delta k_y^2) = [\rho^2+\rho'^2+2\rho\rho'\cos(\phi-\phi')], \tag{16}$$

and Δk_j are Cartesian components of $\Delta\mathbf{k}=\mathbf{k}+\mathbf{k}'-\mathbf{k}_P$. z_0 gives the z position for the minimum waist (focus) of the pump beam. $\mathcal{G}_l^p(\xi)$ is the *polynomial* of order l defined by

$$\mathcal{G}_l^p(\xi) \equiv \sum_{q=0}^{\infty}\frac{(-\xi/2)^q}{q!}{}_2\mathcal{F}_1(-l,1+l+q;1+p;2), \tag{17}$$

and ${}_2\mathcal{F}_1$ is the hypergeometric function [The series (17) reduce to polynomials for specific l values]. $\mathcal{G}_l^p(\xi)$ is easily calculated, for example,

$$\mathcal{G}_0^p(\xi) = e^{-\xi/2},$$

$$\mathcal{G}_1^p(\xi) = e^{-\xi/2}\frac{-3+p+\xi}{1+p},$$

$$\mathcal{G}_2^p(\xi) = e^{-\xi/2}\frac{26+p^2-12\xi+\xi^2+p(-9+2\xi)}{(1+p)(2+p)}. \tag{18}$$

One should observe that the angle φ_k appearing in $e^{-il\ \arctan(\Delta k_y/\Delta k_x)} \equiv e^{-il\varphi_k}$, in Eq. (15), is a global angle connected with the signal *and* idler photons. Being associated with the photon pair it reflects the OAM signature imposed by the pump beam. This point will be further discussed along the paper.

The wave function in Eq. (15) is an improvement over the wave function formerly obtained [13], e.g., in [1]. Insertion of Eq. (15) into Eq. (13) provides the full wave function for SPDC with OAM. Equation (15) has a compact analytical form, is valid for all cases of single photon-pair conversion (Type I or Type II), for all angles allowed by the phase-matching conditions and for all orbital angular momentum values l. Clearly, particular cases can be derived from it including the paraxial cases, most common in the literature.

The conditions that maximize the wave function Eq. (15) are the phase-matching conditions. They give the coordinates (θ,θ') *and* (ϕ,ϕ') that simultaneously maximizes $\tilde{\psi}_{lp}(\Delta\mathbf{k})$ (or the probability amplitude density); they are

$$\frac{\sin[l_c(\Delta k_z/2)]}{[l_c(\Delta k_z/2)]} \to \max(\text{longitudinal condition}), \tag{19}$$

and

$$\xi^{L/2}\mathcal{G}_l^p(\xi) \to \max(\text{transversal condition}). \tag{20}$$

In general, the loci around the maxima are found numerically. They will define the most probable regions where to detect coincident signal and idler photons [14].

Normalization

Normalization of SPDC's wave function is not trivial, despite the apparent simplicity of $\tilde{\psi}_{lp}(\Delta\mathbf{k})$. Each variable Δk_z and ξ specifies two points, each with three coordinates for the signal and idler wave vectors. Numerical integrations of $|\tilde{\psi}_{lp}(\Delta\mathbf{k})|^2$ over the entire volume can be performed for particular cases. While this may the alternative for some applications, it is a demanding procedure.

An order of magnitude for the normalization factor can be obtained with a simplified normalization for $\tilde{\psi}_{lp}(\Delta\mathbf{k})$ (from now on called ξ normalization): assume that the longitudinal phase matching is satisfied, $\sin[l_c(\Delta k_z/2)]/[l_c(\Delta k_z/2)] \sim 1$ and that ξ will span from 0 to ∞, as a compact mapping for the variables $\mathbf{k}$ and $\mathbf{k}'$. This easily leads to

$$\int_0^\infty |\tilde{\psi}_{lp}(\Delta\mathbf{k})|^2 d\xi = |A_{lp}|^2 l_c^2 \pi^2 \times \begin{cases} 4\dfrac{z_R^2}{k_P^2} & (\text{for } l=0), \\ 2[3+(p-2)p]\dfrac{z_R}{k_P} & (\text{for } l=1), \\ \dfrac{(76+p\{-60+p[25+(-6+p)p]\})}{2} & (\text{for } l=2), \\ \cdots \end{cases} . \tag{21}$$

The resulting ξ-normalized probabilities are $P_c \equiv |\tilde{\psi}_{lp}(\Delta\mathbf{k})|^2 / \int_0^\infty |\tilde{\psi}_{lp}(\Delta\mathbf{k})|^2 d\xi$. For $p=0$, it gives

$$P_c = \begin{cases} e^{-\xi} & (\text{for } l=0), \\ \dfrac{1}{3}e^{-\xi}(\xi-3)^2\xi & (\text{for } l=1), \\ \dfrac{1}{152}e^{-\xi}\xi^2[(\xi-12)\xi+26]^2 & (\text{for } l=2), \\ \dfrac{e^{-\xi}(\xi-3)^2\xi^3[(\xi-24)\xi+126]^2}{31752} & (\text{for } l=3), \\ \dfrac{e^{-\xi}\xi^4(\xi\{\xi[(\xi-48)\xi+744]-4320\}+7704)^2}{17\,293\,824} & (\text{for } l=4), \\ \cdots \end{cases} \tag{22}$$

Figure 2 shows plots of P_c for $l=0,1,2,3,4$ as a function of ξ. Also shown are the respective values ξ_l that maximizes each $P_c(l)$. These ξ_l values will impose constraints between ϕ and ϕ' through the transversal phase match condition, Eq. (20).

It may be instructive to see an illustration of the ρ and $\phi-\phi'$ dependence by the normalized wave function [Eq. (15)] for some l values. For example, the dependencies of

$$P_c(l=0,p=0) = |\tilde{\psi}_{00N}(\Delta\mathbf{k})|^2 = e^{-z_R/k_P[\rho^2+\rho'^2+2\rho\rho'\cos(\phi-\phi')]}, \tag{23}$$

and

$$|\tilde{\psi}_{10N}(\Delta\mathbf{k})|^2 = \frac{z_R}{3k_P^3} e^{-z_R/k_P[\rho^2+\rho'^2+2\rho\rho'\cos(\phi-\phi')]} \times [\rho^2+\rho'^2+2\rho\rho'\cos(\phi-\phi')] \times [-3k_P+z_R(\rho^2+\rho'^2)+2z_R\rho\rho'\cos(\phi-\phi')]. \tag{24}$$

are shown in Figs. 3 and 4.

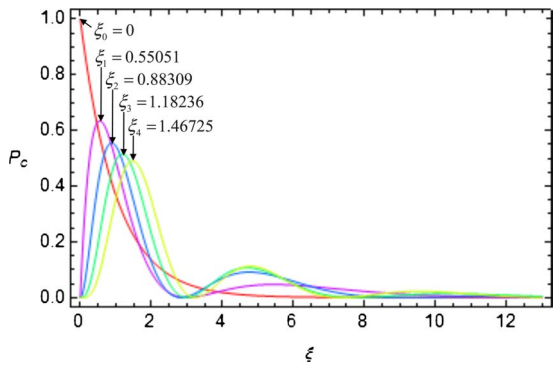

FIG. 2. (Color online) Plots of the coincidence probability of signal and idler photons, P_c, as a function of the dimensionless two-point coordinate ξ, for the OAM values $l=0,1,2,3,4$. P_c has been normalized by the ξ normalization described in the text. Values of ξ_l that maximize P_c are indicated for each OAM l probability curve.

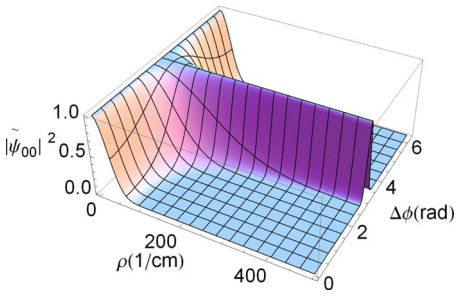

FIG. 3. (Color online) Dependence of the photon-pair probability $|\tilde{\psi}_{00}(\Delta\mathbf{k})|^2$ as a function of ρ and $\Delta\phi=\phi-\phi'$ for a degenerate Type I SPDC. Away from the ρ origin, the photon pair occurs at a narrow range around $\Delta\phi=\pi$. The maximum is on $\Delta\phi=\pi$.

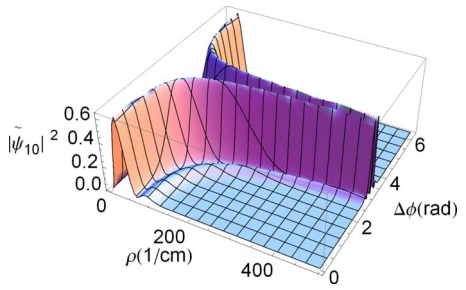

FIG. 4. (Color online) Dependence of the photon-pair probability $|\tilde{\psi}_{10}(\Delta\mathbf{k})|^2$ as a function of ρ and $\Delta\phi=\phi-\phi'$ for a degenerate Type I SPDC. Away from the ρ origin, the photon pair occurs at a narrow range around two values on leafs close to $\Delta\phi=\pi$. There is a minimum on $\Delta\phi=\pi$.

Plotting $|\tilde{\psi}|^2$ on the (k_x,k_y) plane will reveal coincidence structures in the way discussed in Ref. [3]. To do so, one should work around the phase-matching regions, both for the longitudinal and the transverse variables. Comparison with experimental results is then a direct task.

IV. PHASE MATCH

A. Longitudinal match

$\Delta k_z=0$ gives the maximum of the sinc function [see Eq. (19)] and, therefore, the ideal polar phase-matching angles (see Ref. [3] for details). A width measure of the sinc function can be specified, say, by its first minima, given by $|\Delta k_z|=2\pi/l_c$. This gives the maximum and minimum polar angles θ_M and θ_m defining the region within the first maximum of the probability density function is located. All referred angles are internal angles to the optical medium; outside angles are related by Snell's law.

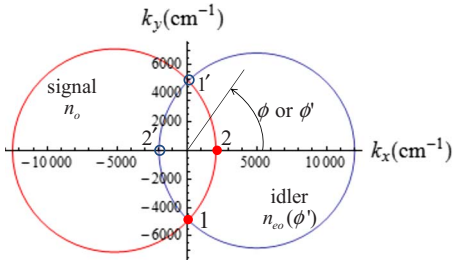

FIG. 5. (Color online) Signal and idler rings for a degenerate Type-II SPDC from a BBO crystal pumped by a laser with wavelength of $\lambda_P=3511$ Å. Points 1 and 1′ are entangled in energy, momentum, and polarization (see Fig. 1). Coincidence structures at the idler positions 1′ and 2′ are calculated ahead, under the assumption that a signal photon was detected at positions 1 and 2, respectively. The signal photons detected are assumed wave vector defined and, therefore, carrying $l=0$. The conjugate idler photons carry OAM l, for a pump beam with OAM l per photon. The OAM value is attached to the photon pair as a whole. The pump beam and its OAM are centered at the origin of the figure and upward from the paper. The laser beam is polarized along the x axis. See a detailed discussion in [3].

Signal and idler rings

The longitudinal condition, Eq. (19), gives for the maximum of the sinc,

$$\Delta k_z=-k_P+[k\cos\theta+k'(\phi')\cos\theta']=0 \tag{25}$$

Similarly as done in [3], a numerical calculation was done for a beta-barium borate crystal searching for coordinate angles that satisfy the longitudinal condition. Parametric conditions can result connecting these angles for the signal and for idler rings,

$$\theta=\arcsin\{\xi_{si}[\cos(\phi-\pi)+\sqrt{\cos^2(\phi-\pi)+\eta_{si}}] + \nu_{si}e^{-\mu_{si}\sin^2[(\phi-\pi)/2]}\}, \tag{26}$$

and

$$\theta'=\arcsin[\xi_{si}(\cos\phi'+\sqrt{\cos^2\phi'+\eta_{si}})+\nu_{si}e^{-\mu_{si}\sin^2(\phi'/2)}], \tag{27}$$

where $\xi_{si}\simeq 0.034\,155\,47$, $\eta_{si}\simeq 0.981\,807\,15$, $\nu_{si}=0.001\,583\,197\,7$, $\mu_{si}=3.084\,419\,87$. All angles use the same coordinate system, where the laser beam is directed along the z axis, coincident with the quantization axis. Figure 5 shows these rings for a BBO crystal pumped by a laser beam with wavelength $\lambda_P=3511$ Å.

Similar parametric equations can be obtained to define the width of the signal and idler rings around each ring given by Eq. (26) and (27). For example,

$$\Delta k_z=-k_P+[k\cos\theta+k'(\phi')\cos\theta']=\pm\frac{\pi}{l_c} \tag{28}$$

may define the ring's "width" or, in other words, the minimum and maximum polar angles where appreciable occurrences of photon pairs will occur.

B. Transversal match

Figure 2 shows the values ξ_l that maximizes P_c. It is easy to perform a numerical search for values of (ϕ,ϕ') that give values ξ close to ξ_l, say within $|\xi-\xi_l|<0.1$. The peak values appear around $|\phi-\phi'|\simeq\pi$ (not at π) for $l\neq 0$ and at $|\phi-\phi'|=\pi$ for $l=0$. These close to diametrically opposed azimuthal values, together with the longitudinal conditions given by Eqs. (26) and (27) completes the necessary information to locate the signal-idler pair in the scattering field.

C. Coincidence plots

A direct writing of ξ in terms of the fundamental variables $(\mathbf{k},\mathbf{k}')$ in P_c, gives the expected coincidence plots shown in Figs. 6–8.

In Ref. [3], similar structures were calculated that show asymmetric donuts. A first-order expansion for the azimuthal angle ϕ' was made around the value $\phi+\pi$, close to the top of the sinc function. This expansion resulted in the asymmetries shown in [3]. Figures 7 and 8 did not use that kind of

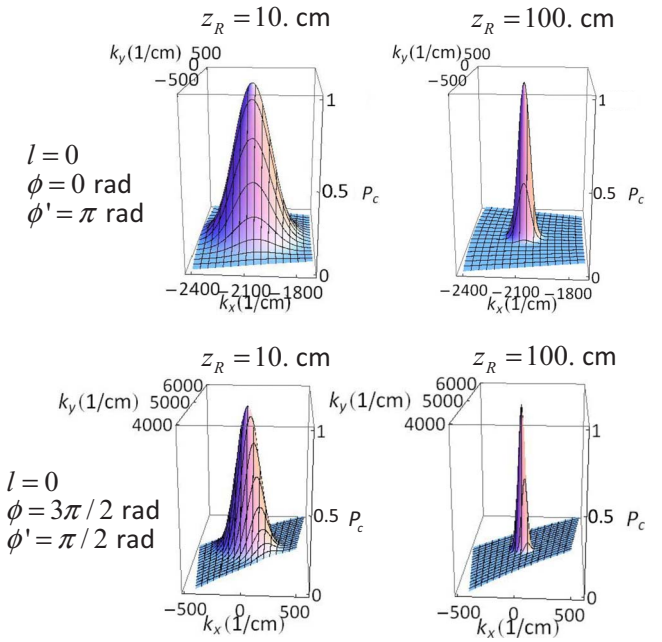

FIG. 6. (Color online) P_c for $l=0$ at different positions for signal and idler detection and different Rayleigh ranges. For each plot, a signal photon has been detected at positions $\phi=0$ rad or $3\pi/2$ rad (positions 1 and 2 in Fig. 5) and P_c describes the detection of an idler photon around $\phi'=\pi$ rad or $\phi'=\pi/2$ rad (positions $1'$ and $2'$ in Fig. 5). A small z_R implies a small laser beam spot and a large scattering region while a large z_R gives a larger spot and a smaller scattering region.

expansion but only the coordinate ϕ' was taken around the same diametrically opposed point $\phi+\pi$. This, together with the use of $\mathcal{G}_l^p(\xi)$, produced the improved coincidence structures shown in Figs. 7 and 8.

The asymmetries seen in [3] were due to equation expansions used around the top of the sinc function (also known as longitudinal phase-matching equation or mismatch equation). However, the similarities between these asymmetries and the published data (see [15]) led to the impression that the used expansion was a reasonable one. These discrepancies show some of the difficulties for comparison of numerical results with noisy data.

It is interesting to observe the effect of varying z_R on Figs. 6–8. A small z_R implies a small beam waist w_0 at the crystal position. A small source produces a large diffraction or scattering region while a large z_R leads to a more concentrated scattering region. These characteristics are clearly seen in these figures. In these figures the OAM values l go from $l=0$ to $l=4$. While donuts present intensity maxima at some finite radius from its center, the $l=0$ has the maximum always centered, in agreement with Fig. 2. For a fixed value of z_R, the donut sizes increase with l, as predicted by Eq. (15) and also seen in Fig. 2.

V. PARTIAL TRANSFER OF OAM BETWEEN PUMP AND SPDC PHOTONS

Some discussion about conservation or nonconservation of OAM in SPDC exists in the literature. Refs. [1,3] discuss this question. The word "conservation" here means complete transfer of OAM from pump to the SPDC photons. It is implicitly assumed that the overall OAM is conserved, what includes the nonlinear medium and all other possible transfer channels. One of the interesting points of the OAM being discussed is that instead of being a quantum feature with integer of half-integer changes, any fractionary change is allowed. One may say that the detected fractionary changes could be analyzed through decompositions of a basis with integer values of OAM. However, there is no evidence of a full quantum character of the OAM associated with light. This is another question yet to be answered conclusively. Nevertheless, partial transfer of OAM is coherent with a classical picture of angular momentum flux conservation across a surface—that is also gauge invariant [16].

A simple calculation will be presented to justify partial OAM transfer or optical nonconservation in some cases and to discuss some questions that could be further clarified. Equation (14) presents a pump mode carrying OAM l that

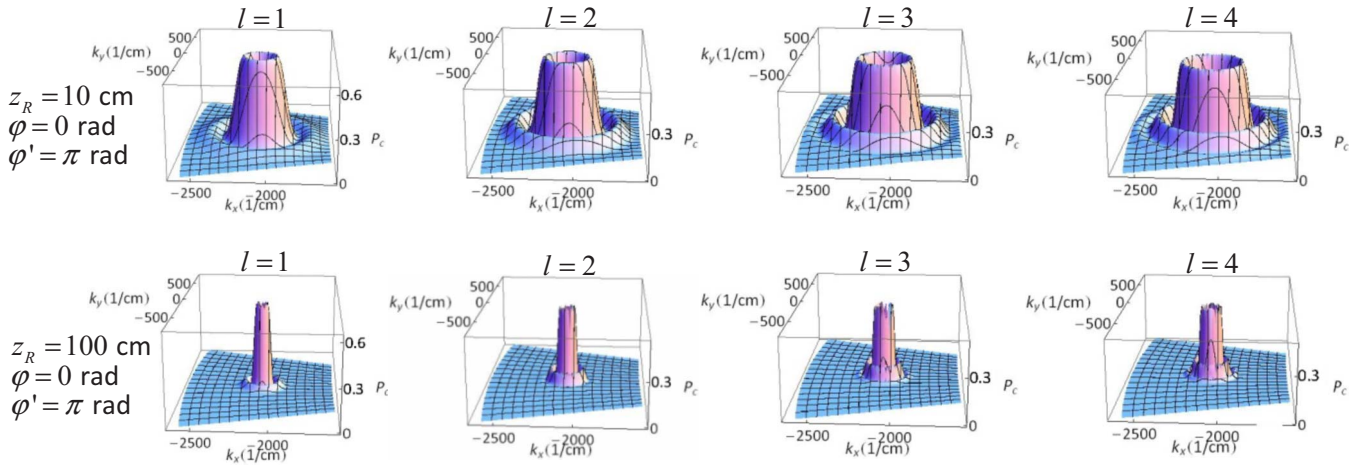

FIG. 7. (Color online) P_c for different l and for $z_R=10$ cm and $z_R=100$ cm. For each plot in top of figure, $z_R=10$ cm and a signal photon has been detected at position $\phi=0$ rad (position 2 in Fig. 5). P_c describes the detection of an idler photon around $\phi'=\pi$ rad (positions $1'$ in Fig. 5). Bottom plots show corresponding figures for $z_R=100$ cm.

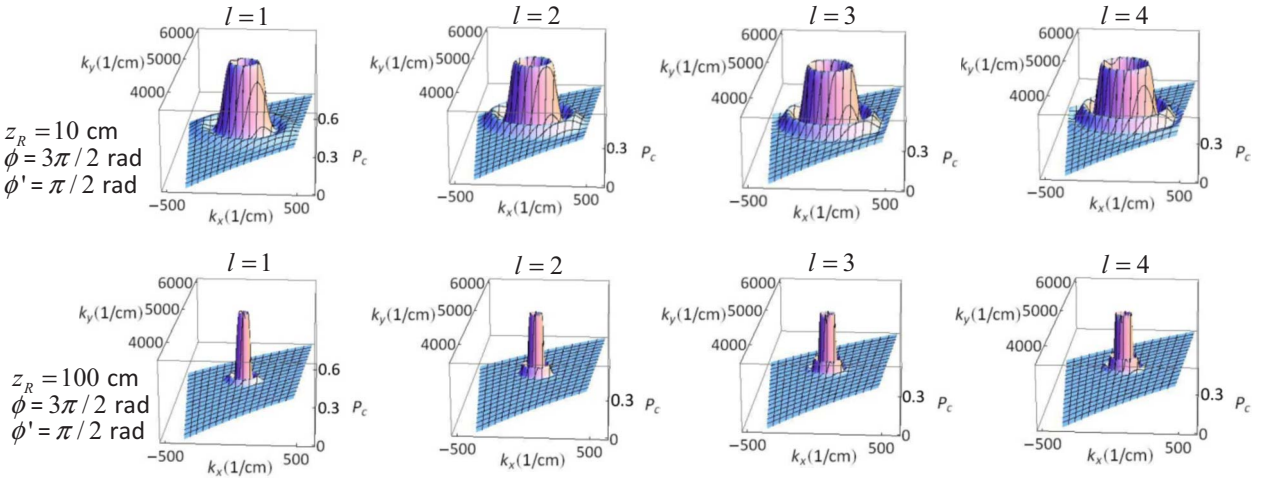

FIG. 8. (Color online) P_c for different l and for $z_R=10$ cm and $z_R=100$ cm. For each plot in top of figure, $z_R=10$ cm and a signal photon has been detected at position $\phi=3\pi/2$ rad (position 2 in Fig. 5). P_c describes the detection of an idler photon around $\phi'=\pi/2$ rad (positions $1'$ in Fig. 5). Bottom plots show corresponding figures for $z_R=100$ cm.

has the phase signature $\exp(il \arctan y/x)$. In SPDC, a photon with OAM l from the pump beam excites the nonlinear medium and its energy decays either as a pump photon or as a pair of photons. Equation (15) shows the wave function connected with this photon pair. The phase signature connected with this photon-pair is given by the term $e^{-il \arctan(\Delta k_y/\Delta k_x)}$. $\Delta k_j (j=x,y)$ is a two-point coordinate related to both signal and idler photons. One could write $\arctan(\Delta k_y/\Delta k_x)=\varphi_k$. This common phase φ_k is related to the photon-pair. If one wants to relate this quantity to the original angles ϕ and ϕ' associated to the signal and idler wave vectors, one just needs to apply the definitions already given to obtain

$$\varphi_k = \arctan \frac{k \sin\theta \sin\phi + k' \sin\theta' \sin\phi'}{k \cos\theta \sin\phi + k' \cos\theta' \sin\phi'}. \tag{29}$$

This global "entangled angle" is not a simple sum of independent angles, such as ϕ and ϕ', but rather an angle associated with the simultaneous propagation of the highly correlated signal and idler photons.

One may call the sum of angles $\phi+\phi'=\Phi_+$ and, correspondingly, $\phi-\phi'=\Phi_-$. Making these substitutions in φ_k one gets

$$e^{-il\varphi_k} \to e^{-il \arctan(k \sin\theta \sin(\Phi_+ + \Phi_-) - k' \sin\theta' \sin(\Phi_+ - \Phi_-)/k \cos\theta \sin(\Phi_+ + \Phi_-) + k' \cos\theta' \sin(\Phi_+ - \Phi_-))}. \tag{30}$$

Considering that an operator for the orbital angular momentum along the z axis could be written $\hat{L}=\pm i\hbar \frac{\partial}{\partial \Phi_+}$ or $\hat{L}=\pm i \frac{\partial}{\partial \Phi_-}$, it is easy to see that (make $\hbar=1$:)

$$i\frac{\partial}{\partial \Phi_+} e^{-il\varphi_k} = l e^{-il\varphi_k}, \tag{31}$$

and

$$i\frac{\partial}{\partial \Phi_-} e^{-il\varphi_k} \neq l e^{-il\varphi_k}, \tag{32}$$

what may lead to the impression that OAM could be conserved for Φ_+ but not for Φ_-. In fact,

$$\tilde{\psi}_{lp}(\Delta\mathbf{k}) = |\tilde{\psi}_{lp}(\Delta\mathbf{k})| e^{-il\varphi_k}, \tag{33}$$

and even for Φ_+ conservation exists only if $|\tilde{\psi}_{lp}(\Delta\mathbf{k})|$ does not depend on Φ_+. However, in general, $|\tilde{\psi}_{lp}(\Delta\mathbf{k})| = |\tilde{\psi}_{lp}(\phi,\phi')|$ depends on the azimuthal angles. Only for certain cases, such as Type I SPDC, where both signal and idler refractive indices do not depend on these angles OAM transfer could be perfect. Refractive indices are implicitly attached to the wave vector magnitudes k [e.g., $k=(2\pi/\lambda)n$] and k'. This reasoning was presented in Ref. [1]. In all cases where the interaction processes in the medium lacks azimuthal symmetry (and, therefore, $|\tilde{\psi}_{lp}(\Delta\mathbf{k})|$ as well), OAM will not be fully transferred to the photon pairs.

It is also interesting to see that, e.g., for the particular case $k=k'$ and $\theta=\theta'$ one has $\varphi_k=\Phi_+/2$. This is the simplest case connecting the global angle φ_k to the signal and idler angles. It is also the degenerate Type I down-conversion case. On the other hand, in general, Type II down conversion seems to fail to present a perfect OAM transfer. One question still not satisfactorily answered is "where are the confirmations for this prediction of a partial OAM transfer?"; some discussion on this question continues ahead.

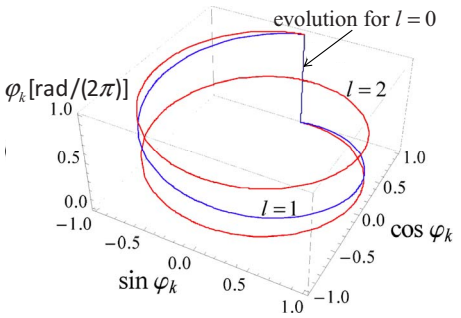

FIG. 9. (Color online) One period of a helix traced by phase advance of φ_k for distinct values of l.

Figure 9 shows a single period of helices traced by variation of φ_k for different values of $l(l=0,1,2)$. It should be emphasized that φ_k is associated with the photon pair as a whole.

Conservation of OAM ($\Delta l=0$) from pump to the SPDC photons, as discussed in Refs [1]. demands maximum *uncertainty* ($\Delta\phi\rightarrow 2\pi$) in the specification of the azimuthal angles ϕ or ϕ' (or Φ_+ and Φ_-) at any instant. Consequently, as the photon-pair propagates their azimuthal angle correlation $\langle\phi(t)\phi'(t+\tau)\rangle=\langle\phi(0)\phi'(\tau)\rangle$ should be independent of the time (or position) where the correlation was measured. This should happens regardless the specific values of ϕ or ϕ', reflecting azimuthal symmetry. For example, in degenerate Type I down conversion, for a photon detected at the azimuthal angle ϕ, its pair will be detected at the angle $\phi+\pi$. In this case both photons propagate inside the nonlinear medium with the same speed, with equal linear refractive indices for both photons. At any time this correlation will be obeyed, due to momentum conservation. In the other way, for Type-II down conversion the signal and idler photons see different refraction indices and, therefore, their spatial correlation are modified with time. This is at the source of the incomplete transfer of OAM from the pump photons to the SPDC's photon pair. As has been widely demonstrated, although the OAM is not a true quantum orbital angular momentum, the OAM l associated to a laser beam can even be transferred to independent macroscopic particles and the transferred momentum can be measured (for example, see [17]).

In the cases when the SPDC photon pair is not carrying the initial OAM l associated to the pump photon but only a partial OAM l_f, a pertinent question is: where $\Delta l=(l-l_f)$ went? Next section discusses this problem.

VI. OAM DECAY CHANNEL

What could be the decay channel for the OAM $\Delta l=(l-l_f)$? The Hamiltonian (12) contains some information on the linear and the nonlinear characteristics of the medium in parametric form: linear refractive indices n and n' and the nonlinear χ. This parametric information has not led to a clear answer to this question up to now. As discussed, the different propagation times for signal and idler photons should produce a spatial dephasing of the photons and the incomplete OAM transfer.

Is the Hamiltonian given by Eq. (12) capable of explaining the partial OAM transfer in detail? Its Hermitian character does not allow any absorptive processes unrelated to a fast decay following the absorption. In case OAM decays to the medium, Eq. (12) does not have channels to explain it. Therefore, although macroscopic assumptions can be *ad-hoc* imposed to achieve some understanding in terms of the distinct propagation times for signal and idler photons, it is not clear that a full understanding could be obtained only from Eq. (12). It seems natural to ask what ingredients could be missing for a full explanation.

One may start asking what measurable effects would appear with a partial OAM transfer. Some possibilities are:

(1) The coincidence probabilities may show signatures of partial transfer of OAM. In case some processes with distinct l values may occur, characteristic donuts should appear, in pure or mixed form. For example, for $l=0$ and $l\neq 0$, Gaussian occurrences could partially fill the donut centers seen in Figs. 7 and 8 ($l\neq 0$). The relative weight between the donut probability ($l\neq 0$) and the Gaussian events ($l=0$) will produce a *measure* of the nontransferred part $\Delta l=l-l_f$. In this case, $P_c=\alpha_0 P_c(l=0)+\alpha_l P_c(l\neq 0)$, where $\alpha_0+\alpha_l=1$. α_j are the associated weights.

(2) SPDC experiments performed with the nonlinear medium mounted on a magnetically levitated support, may reveal directly Δl through the succession of the microscopic time-random down-conversion events adding microscopic torques $\tau(t_i)$ to the nonlinear medium $\Delta l=\Sigma_i\tau(t_i)\Delta t_i$. The system could be mounted on a interferometric setup for increased resolution.

(3) The energy from the pump excited medium could decay through the lattice, producing lattice excitations compatible with the transferred OAM. In this case, rotorlike excitations or particular anti-Stokes phonons with modes compatible with the OAM properties may be detected at low temperatures signaling OAM decay.

These possibilities suggest, as a speculation, that the standard Hamiltonian (12) could be modified to increase the microscopic understanding of these OAM decay channels. However, this task is expected to be very demanding, but not untreatable. The first difficulties to be found to track down the OAM "losses" through a microscopic analysis relate to: (a) the way the pump laser field couples to the nonlinear medium and, (b) the way that the photon-pair field(s) propagates through the medium. Both χ and the linear refractive indices n and n' are just concise "response functions" of the medium representing the complex microscopic behavior of the condensed matter. As known, the Kramers-Kronig (KK) relationships [9] show that even under the assumption of real linear and nonlinear susceptibilities (e.g., $\chi^{(1)}=\chi^{(1)'}$ and $\chi^{(2)}=\chi^{(2)'}$), there are corresponding imaginary contributions given by $\chi^{(1)''}$ and $\chi^{(2)''}$. For example, a real susceptibility

$$\chi' \propto \left(\frac{1}{\omega+\omega_1}-\frac{1}{\omega-\omega_1}\right), \tag{34}$$

would lead to

$$\chi'' \propto [\delta(\omega-\omega_1)-\delta(\omega+\omega_1)], \tag{35}$$

expressing an absorption or re-emission process. These connections are determined by causality.

Among possible microscopic descriptions for the involved physical phenomena one could start, for example, by the very fast ($\Delta t \to 0$) absorption of pump light with energy within the band gap of the insulator medium. This absorption could proceed through absorption of the energy by virtual electrons in the medium followed by their fast decay. This fast process implies that the uncertainty in the energy, ΔE, is large enough to allow the fast excitation of electronic levels establishing an instantaneous polarizability of the medium (see [3]). The fast electronic decay could proceed either giving back the energy as pump photons, or as photon pairs, to optical phonons due to electron-phonon coupling or even to some rotorlike excitation. It is to be wondered if phonon excitations could lead to rotorlike excitation with a given OAM vector. In the case of energy decay to phonons (optical or acoustic phonons) the associated energy will be initially transferred as mechanical vibration modes of the lattice (or even as polaritons, the mixed light-mechanical mode). Due to anharmonic phonon-phonon coupling the energy could end up as heat associated to the lattice. After an initial modeling including electronic interactions, the virtual electrons should be traced out leading to effective response functions or susceptibilities $\chi^{(1)}_{eff}$, $\chi^{(2)}_{eff}$.

The understanding of OAM losses by the medium, could be attempted by adding terms to the Hamiltonian (12) representing virtual electrons, phonons, and other excitations and their coupling. This is an open problem at this moment. To avoid the daunting task of a perfect follow up of these microscopic channels, simplified ideas have been applied with success to other processes, such as Raman scattering in dielectric crystals. In this case, where the excitation pump energy is well within the transparent band gap of the insulator medium [18], a simplified model derives electron and phonon response functions that gives good agreement with experiments. It would be very rewarding if this problem could be solved by some simple argument.

The main message here is to state that a fine understanding of transfer of OAM to the SPDC photons has not been achieved yet, despite some effort to do so. As always, advance in the understanding of fundamental process could bring valuable rewards. Again, further experimental efforts could provide the best guidance toward a full understanding of partial OAM transfer.

VII. CONCLUSIONS

This paper improves the wave function for SPDC with OAM discussed in [1], [3], and related literature. This improved wave function, Eq. (13), is written in terms of the wave vectors (**k** space), nonlinear and linear medium parameters and the laser beam specifications. Examples of the probability density for coincident photon events, or conjugated photon pairs, were given for Type-II SPDC. This wave function has a compact form useful for numerical estimates. It may also allow further analytical advances such as integration over the wave vector variables and even to perform Fourier transforms aimed to obtain the complete wave function in the **r** space. Wave functions written in the **r** space could be particularly useful for measurements of photon-pair correlations at the source itself [5]. Furthermore, these global wave functions are expected to have full applicability for parallel detection of the emitted photon pairs in all allowed angles for SPDC. Partial transfer of OAM from the pump photons to the SPDC photon pairs was further discussed, stressing that without optical azimuthal symmetry of the medium a full transfer is not allowed. Possible improvements of the wave function starting from modified Hamiltonians are also indicated to include microscopic channels for OAM decay. It is also recognized that signatures of this partial transfer have not yet been demonstrated, other than theoretical indications that lack of azimuthal symmetry does not allow the wave function to be an eigenstate of the orbital angular momentum operator. Some conjectures were forwarded about how to observe experimentally the partial transfer. Further theoretical and experimental work may help clarify this fundamental problem. The reader is stimulated to contribute in this development.

ACKNOWLEDGMENT

This work was supported by the U. S. ARO MURI Grant No. W911NF-05-1-0197 on Quantum Imaging.

APPENDIX: CALCULATION OF $\tilde{\psi}_{lp}(\Delta\mathbf{k})$

In cylindrical coordinates, $\tilde{\psi}_{lp}(\Delta\mathbf{k})$ is

$$\tilde{\psi}_{lp}(\Delta\mathbf{k}) = \int_{z_0-l_c/2}^{z_0+l_c/2}\int_0^\infty\int_0^{2\pi} e^{-i(\Delta k_x\rho\cos\phi+\Delta k_y\rho\sin\phi)+\Delta k_z z} \times \tilde{\psi}_{lp}(\Delta\mathbf{k})\rho d\phi d\rho dz \tag{A1}$$

Azimuthal integral

Integration on the azimuthal angle $\phi=\arctan y/x$ is given by I_ϕ

$$I_\phi = \int_0^{2\pi} e^{-i(\Delta k_x\rho\cos\phi+\Delta k_y\rho\sin\phi)} e^{-il\phi} d\phi. \tag{A2}$$

This integral can be found in Ref. [19], giving

$$I_\phi = 2\pi\frac{(\Delta k_x - i\Delta k_y)^l}{(\Delta k_x^2+\Delta k_y^2)^{l/2}} e^{-iL\pi/2} J_l(-\rho\sqrt{\Delta k_x^2+\Delta k_y^2}). \tag{A3}$$

Therefore, $\tilde{\psi}_{lp}(\Delta\mathbf{k})$ is written

$$\tilde{\psi}_{lp}(\Delta\mathbf{k}) = \int_{z_0-l_c/2}^{z_0+l_c/2} e^{-i\Delta k_z z} 2\pi\frac{z_R A_{lp}(k_P/\sqrt{2})^l}{(z_R^2+z^2)^{(l+1)/2}} \times e^{i[(2p+l+1)\arctan(z/z_R)-l\pi/2]}\frac{(\Delta k_x - i\Delta k_y)^l}{(\Delta k_x^2+\Delta k_y^2)^{l/2}} \times \left[\int_0^{2\pi}\rho^{l+1}L_l^p\left(\frac{z_R k_P}{z_R^2+z^2}\rho^2\right)e^{-i[(k_P z\rho^2/2)/(z^2+z_R^2)]}\right.$$

$$\times e^{-[(k_P z\rho^2/2)/(z^2+z_R^2)]} J_l[-\rho\sqrt{\Delta k_x^2+\Delta k_y^2}]d\rho\Bigg]dz. \quad \text{(A4)}$$

The series representation of the Laguerre function

$$L_l^p\left(\frac{z_R k_P}{z_R^2+z^2}\rho^2\right)=\sum_{r=0}^{l}(-1)^r\binom{l+p}{l-r}\frac{\left(\frac{z_R k_P}{z_R^2+z^2}\rho^2\right)^r}{r!} \quad \text{(A5)}$$

can be used: Including the term in ρ^{2r}, in the ρ integral within brackets (call it I_r) in Eq. (A4), a solution is given by *Mathematica*,

$$\begin{aligned} I_r &\equiv \int_0^{2\pi}\rho^{l+1+2r}e^{-i[(k_P z\rho^2/2)/(z^2+z_R^2)]} \\ &\times e^{-[(k_P z\rho^2/2)/(z^2+z_R^2)]}J_l(-\rho\sqrt{\Delta k_x^2+\Delta k_y^2})d\rho \\ &= \frac{(-1)^l 2^r\Gamma(1+l+r)}{\Gamma(1+l)}(\Delta k_x^2+\Delta k_y^2)^{l/2}\left(\frac{k_P}{z_R-iz}\right)^{-l-r-1} \\ &\times {}_1F_1\left[l+r+1,l+1;\frac{(-zR+iz)(\Delta k_x^2+\Delta k_y^2)}{2kP}\right] \end{aligned} \quad \text{(A6)}$$

Therefore,

$$\begin{aligned} \tilde{\psi}_{lp}(\Delta\mathbf{k}) &= \int_{z_0-l_c/2}^{z_0+l_c/2}\frac{2\pi(-1)^l}{\Gamma(1+l)}\frac{A_{lp}z_R(k_P/\sqrt{2})^l}{(z_R^2+z^2)^{(l+1)/2}} \\ &\times e^{i[(2p+l+1)\arctan(z/z_R)-l(\pi/2)-\Delta k_z z]} \\ &\times(\Delta k_x-i\Delta k_y)^l\left(\frac{k_P}{z_R-iz}\right)^{-(1+l)}\sum_{r=0}^{l}\binom{l+p}{l-r} \\ &\times\Gamma(1+l+r)\frac{[(-2z_R(z_R+iz))/(z^2+z_R^2)]^r}{r!} \\ &\times {}_1F_1\left[1+l+r,1+l;\frac{\Delta k_x^2+\Delta k_y^2}{2k_P}(iz-z_R)\right]dz. \end{aligned} \quad \text{(A7)}$$

Instead of trying to solve the z integral for a general case, one could observe that the involved z range, Δz, goes from $z_0-l_c/2$ to $z_0+l_c/2$, giving $\Delta z=l_c$. The condition $\Delta z \ll z_R$ is easily achievable in the laboratory, covers most of the cases treated so far, and gives directly the solution in Eq. (15).

Equation (15), therefore, supersedes all approximations formerly used, e.g., in Ref. [1] and so on. Although qualitative dependencies of the variables in the Eq. (15) and former calculations are similar and the resulting numerical longitudinal phase-matching conditions are the same, coefficients of the polynomials in the transverse variable ξ are different.

[1] H. H. Arnaut and G. A. Barbosa, Phys. Rev. Lett. **85**, 286 (2000).

[2] S. Franke-Arnold, S. M. Barnett, M. J. Padgett, and L. Allen, Phys. Rev. A **65**, 033823 (2002).

[3] G. A. Barbosa, Phys. Rev. A **76**, 033821 (2007).

[4] S. Feng and P. Kumar, Phys. Rev. Lett. **101**, 163602 (2008). This reference predicts that photons could be detected on a circle around a point on the down-conversion ring as shown in their Fig. 2. This would constitute a "decay" channel for OAM. However, this "scattering" geometry is *not* allowed by phase matching according to the Fresnel's equations and the accepted Sellmeier's parameters, what invalidates their prediction: as Fresnel's equations are directly derived from Maxwell's equations, their model is in direct conflict with these honorable equations.

[5] H. Di Lorenzo Pires and M. P. van Exter, Phys. Rev. A **79**, 041801(R) (2009).

[6] W. H. Louisell, A. Yariv, and A. E. Siegman, Phys. Rev. **124**, 1646 (1961); D. Magde and H. Mahr, *ibid.* **171**, 393 (1968); G. T. Giallorenzi and C. L. Tang, *ibid.* **166**, 225 (1968); B. Ya. Zel'dovich and D. N. Klyshko Pis'ma Zh. Eksp. Teor. Fiz. **9**, 69 (1969) [JETP Lett. **9**, 40 (1969)]; D. C. Burnham and D. L. Weinberg, Phys. Rev. Lett. **25**, 84 (1970).

[7] C. K. Hong and L. Mandel, Phys. Rev. Lett. **56**, 58 (1986); L. J. Wang, X. Y. Zou, and L. Mandel, Phys. Rev. A **44**, 4614 (1991); T. E. Keller and M. H. Rubin, *ibid.* **56**, 1534 (1997); W. P. Grice and I. A. Walmsley, *ibid.* **56**, 1627 (1997).

[8] Irreversible deformations are associated with crystal damage, a non-negligible factor in several experiments with intense pumps.

[9] J. D. Jackson, *Classical Electrodynamics*, 2nd ed. (Wiley, New York, 1975).

[10] The polar character of the polarization implies that, under inversion upon a symmetry center, **P** would be transformed to **−P**. The second-order polarizability, depending on E^2, implies that $\chi^{(2)}=0$ in these crystals.

[11] L. Mandel and E. Wolf, *Optical Coherence and Quantum Optics* (Cambridge University Press, New York, 1995).

[12] L. Allen, M. W. Beijersbergen, R. J. C. Spreeuw, and J. P. Woerdman, Phys. Rev. A **45**, 8185 (1992).

[13] $e^{\xi/2}\mathcal{G}_l^p(\xi)$ was mistakenly identified as $L_l^p(\xi)$ in Ref. [1]. They are polynomials of the same order and have similar ξ dependences but they have different coefficients.

[14] Speculations exist in the literature that point to different locations for some occurrences of photons from SPDC. However, occurrences that are not at or very close to the ideal phase match conditions (as defined in the present paper) are extremely improbable. As a word of caution, poor expansions of phase-matching equations or use of nonrepresentative numerical approximations for Sellmeier's equations lead to ill results. Our numerical phase-matching rings are consistent with the experimental results and no other region over the scattering region should present a non-negligible occurrence of signal and idler photons.

[15] S. Feng, C.-H. Chen, G. A. Barbosa, and P. Kumar, e-print arXiv:quant-ph/0703212.
[16] S. M. Barnett, J. Opt. B: Quantum Semiclassical Opt. **4**, S7 (2002).
[17] A. T. O'Neil, I. MacVicar, L. Allen, and M. J. Padgett, Phys. Rev. Lett. **88**, 053601 (2002).
[18] A. S. Barker, Jr. and R. Loudon, Rev. Mod. Phys. **44**, 18 (1972).
[19] W. Gröbner and N. Hofreiter, *Integraltafel* (Springer Wien, New York, 1961), p. 144.